Experimental study of sensitivity enhancement in SPR biosensors by use of zinc oxide intermediary layers

Nan-Fu Chiu[1]*, Amit Singh[2], Nathan Nelson-Fitzpatrick[2], Sarang Dutt[2], Stephane Evoy[2+], Chii-Wann Lin[3#]

[1]Institute of Electro-Optical Science and Technology, National Taiwan Normal University, Taiwan, * nfchiu@ntnu.edu.tw
[2]Department of Electrical and Computer Engineering, National Research Council-National Institute for Nanotechnonology, University of Alberta, Canada, + evoy@ece.ualberta.ca
[3]Institute of Biomedical Engineering, National Taiwan University, Taiwan, # cwlinx@ntu.edu.tw

ABSTRACT

We report a novel design for the intermediary layer of surface plasmon resonance (SPR) devices that use high refractive index and high-transmittance zinc oxide (ZnO) dielectric layers to enhance the signal quality and improve the full width at half-maximum (FWHM) of the reflectivity curve. We optimized the design of ZnO thin films using different sputtering parameters and performed analytical comparisons with conventional intermediary layers of chromium (Cr) as well as indium tin oxide (ITO). The study is based on application of the Fresnel equation, which provides an explanation and verification for the observed SPR narrow-width curve and optical transmittance spectra displayed by (ZnO/Au)-1, (Cr/Au)-4 and (ITO/Au)-5 devices. On exposure to ethanol, the (ZnO/Au)-1 device showed a two-fold decrease in FWHM and a 4.5-fold larger shift in intensity interrogation. The (ZnO/Au)-1 device exhibits a wider linearity range and much higher sensitivity. They also exhibit a good linear relationship between angle and concentration dependence in the tested range. We show that these advances represent a novel and simple method for preparing high-sensitivity, high-resolution SPR biosensors for accurate and specific bio-molecular detection.

Keywords: Intermediary layer, surface plasmon resonance (SPR), zinc oxide (ZnO), refractive index unit (RIU), Full Width at Half-Maximum (FWHM), angular interrogation mode, intensity interrogation mode, biosensor.

1 INTRODUCTION

Surface plasmon resonance (SPR) is an evanescent guided electromagnetic wave mode that propagates along a metal-dielectric interface [1-3]. It is known that high-density electron gas, when subjected to collective longitudinal excitations, will exhibit particle behavior. This phenomenon was first observed in the early 1900s, with respect to the transfer of light energy (photons) to a group of electrons (plasmon) on a metal grating surface [4]. Since then, Kretschmann and Otto prism-coupling devices have been used extensively to study the optical properties of metallic thin films, including index of refraction (n), extinction coefficient (k), thickness (d), and roughness [5,6]. Conventionally, SPR biosensors make it possible to detect biomaterial concentration, thickness, and specific biological analytes.

In the traditional attenuated total reflection (ATR) method, a prism-based SPR sensing chip configuration is used, generally with gold (Au) deposited on either a chromium (Cr) or titanium (Ti) adhesion layer (2~5 nm). These Cr/Au and Ti/Au films both exhibit large full width at half maximum (FWHM) values of about three degrees for incident light of 632 or 658 nm wavelength [7-9]. However, this method introduces several problems involving metal interdiffusion and low optical transmission to the gold surface [10,11]. Other new SPR devices have been shown to improve the plasmon efficiency, including active plasmonic coupled emission [12-14], prism-based coupler periodic metallic nanostructures [15] and multi-layer devices [16]. Recently, enhancement of SPR characterization of germanium (Ge) semiconductor films by Si prism-based technology [17] and conducting metal indium tin oxide (ITO) has been reported [18,19]. Therefore, the development of more ideal materials may be the innovation required in biosensor substrates to increase detection sensitivity.

As a semiconductor material, ZnO thin films exhibit excellent optical and electrical properties including high refractive index, high transparency, and low resistivity [20,21]. Many studies have been carried out exploring ZnO nanostructure with Au nanoparticles [22-25] because of the ability of ZnO thin films to enhance optical properties in SPR. In our previous report, we have demonstrated the high-sensitivity detection of CA15-3 for breast tumor marker [26]. The results show that an Au/ZnO SPR offers a potentially powerful assay. Consequently, we consider the optimal design of the intermediary layer to improve the SPR efficiency of the narrow-width curve.

2 MATERIALS AND METHODS

[1] Institute of Electro-Optical Science and Technology, National Taiwan Normal University, No. 88, Sec. 4, Ting-Chou Road, Taipei, 11677 Taiwan, Ph: 886-2-77346731, Fax:886-2-86631954, nfchiu@ntnu.edu.tw

Our SPR reflectivity curve was generated with an intermediary layer SPR device, such as a glass-dielectric-metallic-dielectric (test fluid medium) interface. This process reveals that the different resonance angles observed were due to different interfaces. A surface plasmon consists of an evanescent wave field, the resonance of which is absorbed by free electrons contained in the thin metal film, as shown in Figure 1(a). In general, the metal films use gold (Au) because of its excellent chemical resistance and high extinction coefficient (*k*). As shown in Figure 1(b), Cr is highly reflective and has a high extinction coefficient (*k*) [27,28]. In this paper, we fabricated five different intermediary thin film devices, which include three kinds of zinc oxide/gold (ZnO/Au) devices and one each with chromium/gold (Cr/Au) and indium tin oxide/gold (ITO/Au). We consider the optimal design of the ZnO thin films with respect to increases in transmittance and refractive index and improvement in the FWHM of the SPR reflectivity curve. Compared to conventional SPR devices, these devices yield a considerably narrower SPR feature through the use of a laser light source on a coupling SF10 prism (refractive index n =1.72, 3 × 3 cm^2, 60-degree angle, Edmund Optics, Inc.) with dripped match oil (n) 1.72±0.005 at 25°C (R. P. Cargille Laboratories, Inc.).

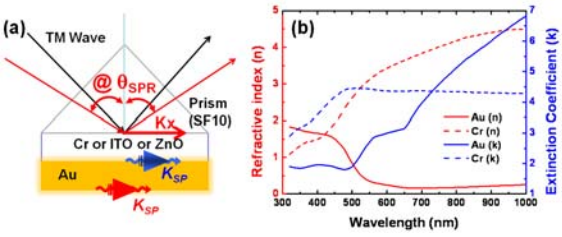

Figure 1. (a) Kreschmann configuration of a four-layered SPR system consisting of prism glass, an intermediary layer, gold film and test fluid medium. (b) UV-vis-NIR spectra to determination the effective refractive index of Au with Cr.

2.1 Fabrication of intermediary layer

In order to find the optimum conditions for coupled narrower SPR, we fabricated three different ZnO thin films varying sputter power and substrate temperature control. The ZnO thin films were grown using a radio frequency (RF) 13.56 MHz sputtering system (ULVAC Japan Inc.). A metallic Zn (99.99%) target was used for ZnO deposition. The films were grown at three different temperatures (200, 150, and 25°C) for (ZnO/Au)-1, (ZnO/Au)-2, and (ZnO/Au)-3 devices, respectively, with the RF power control at 200 W for (ZnO/Au)-1 and 150 W for (ZnO/Au)-2 and (ZnO/Au)-3 devices. A working pressure of 3 mTorr was employed during the deposition and the working gas was a mixture of Ar (40%) and O_2 (30%) gas. In addition, we tried to demonstrate the effectiveness of crystal orientation ZnO (002) growth control and made comparisons of parameters involved in the deposition process for the optimization of our rf-sputtered ZnO thin films. We fabricated (Cr/Au)-4 and (ITO/Au)-5 for comparison. The (Cr/Au)-4 film consists of a 2 nm Cr (99.5%) layer deposited by electron beam evaporator. For the (ITO/Au)-5 device, the substrate thickness is 0.7 mm comprises 200 nm of ITO thin film with a sheet resistance of 46.6 Ω/□ (Merck & Co., Inc.). The 50 nm Au (99.95%) films were deposited by an electron beam evaporator at a vacuum level of about 3×10^{-6} Torr, with an evaporation rate of approximately 0.2 Å/s.

3 RESULTS AND DISCUSSION

3.1. Comparisons of the ZnO crystal (002) orientation and the SPR reflectivity curve

In this work, we consider optimal design problems with multiple objectives. We used an intermediary layer of ZnO thin film to improve the sensitivity and detection limit of surface plasmon resonance. Figure 2 shows X-ray diffraction (XRD) (Nonius, Kappa CCD Single Crystal XRD) results obtained with the ZnO/Au thin films prepared on glass slides by rf-sputtering at different temperatures. The first thing to notice in the XRD results is the relative peak intensity of the ZnO orientation (002). The ZnO thin films growth characterization is kinetic energy of the ions assisted deposition on glass substrates. The strongly (002) oriented ZnO film resulted in a higher kinetic energy, brought about by the higher density of Zn atoms along the (002) plane. We observed that the crystalline (002) orientation improved, showing a decrease in the FWHM of SPR angle. It is because the increase in RF power and substrate temperature enhances the growth density of the ZnO thin film.

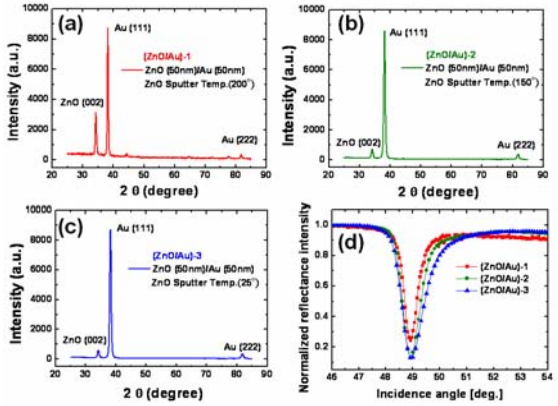

Figure 2. XRD patterns exhibited by ZnO thin films deposited on glass under different conditions. (a)-(c) show the diffraction angle (2θ), the FWHM and the peak intensity of X-ray diffraction of the three sample devices; (d) shows their SPR reflectivity curves.

We analyzed the three ZnO/Au device configurations and evaluated their performances. Figures 2(a), (b), and (c) show XRD patterns which exhibit three peaks corresponding to the (002) plane of ZnO and (111) and (222) planes of the Au films. These XRD results show that (ZnO/Au)-1 is better than (ZnO/Au)-2 and (ZnO/Au)-3 for SPR biosensor purposes because (ZnO/Au)-1 possesses a strong (002) orientation diffraction intensity. We can see that the ratio of the (002) diffraction maximum intensities

of (ZnO/Au)-1:(ZnO/Au)-2:(ZnO/Au)-3 is 5.4:1.2:1. We measured and compared the (002) diffraction peak intensity and the FWHM of the SPR curves of the three sample devices. Figure 2(d) shows that the SPR reflectivity curve of (ZnO/Au)-1 is better than that of (ZnO/Au)-2 and (ZnO/Au)-3; (ZnO/Au)-1 has a narrower SPR curve. The FWHM of the SPR reflectivity curve of the (ZnO/Au)-1, (ZnO/Au)-2 and (ZnO/Au)-3 devices are 0.551, 0.779 and 0.898 degrees, respectively. The SPR curve pattern shows that the parameters of the (ZnO/Au)-1 device are optimal.

3.2. Comparisons of optical properties and surface morphology

Figure 3(a) shows the transmittance spectra of the devices. The spectra of the (ZnO/Au)-1, (ZnO/Au)-2, (ZnO/Au)-3, (Cr/Au)-4, and (ITO/Au)-5 devices show maximum transmittance peaks at 513, 513, 509, 501, and 506 nm, respectively; all of which fall within the green light wavelength region. We are interested in the entire transmittance spectrum (400-600 nm) of visible light because this represents the SPR range when the incident light wavelength range is between 780-833 nm. We can use the dispersion relation of the ZnO/Au and Au/test fluid medium interface to calculate the surface plasmon wavelength, as shown by Eq. (1) [29]:

$$\lambda_{SP(ZnO/Au)} = \frac{2\pi}{k_{sp}} \approx \lambda_0 \sqrt{\frac{\varepsilon_{ZnO} + \varepsilon_{Au}}{\varepsilon_{ZnO}\varepsilon_{Au}}}, \quad and \quad \lambda_{SP(medium/Au)} \approx \lambda_0 \sqrt{\frac{\varepsilon_m + \varepsilon_{Au}}{\varepsilon_m \varepsilon_{Au}}} \qquad (1)$$

where λ_{SP} is the wavelength of SPR resonant light, k_{SP} is the surface plasmon wave vector parallel to the surface, ε_m, ε_{ZnO} and ε_{Au} are the dielectric constants of the test fluid medium, ZnO and Au, respectively, and λ_0 is the wavelength of the excitation light in a vacuum.

The (ZnO/Au)-1, (ZnO/Au)-2 and (ZnO/Au)-3 devices show high transparent properties relative to the (Cr/Au)-4 and (ITO/Au)-5 devices. The (Cr/Au)-4 and (ITO/Au)-5 devices exhibited lower transparency due to high reflection and absorption by the intermediary Cr [28] and ITO [30-32] layers. In the average visible light region, transmittance by ITO and ZnO thin films is about 80% and 90%, respectively.

The refractive index and extinction coefficient were evaluated for the ZnO, Cr and ITO thin films using an EP^3 imaging ellipsometer. We used previous [33] studies to measured and estimated the optical properties of various densities. The measured data were fit to the best optical parameters of the samples. The dispersion of the oxide layer was assumed to follow that of ZnO and ITO films based on the Cauchy model and the Lorentz oscillator model, respectively [34]. Figure 3(b) shows the refractive indices of ZnO, Cr and ITO measured at 833, 643 and 532 nm, respectively. Data on the refractive index of Cr, ZnO and ITO films from previously published work [28,34,35] are included for comparison (solid line in the figure). It can be seen that the refractive index shows dependency on wavelength. The (ZnO/Au)-1 device has a high refractive index of 1.96, 1.96 and 1.97 at wavelengths of 833, 643 and 532 nm, respectively. The refractive indices of (ZnO/Au)-1, (Cr/Au)-4 and (ITO/Au)-5 devices at 833 nm wavelength are 1.96, 4.4 and 1.53, respectively; values that are close to those calculated from the technical literature, as shown in Fig. 3(b). In Table 1, it can be seen that the refractive index of ZnO films increases from 1.93 to 1.96 with increasing substrate temperature from 25 to 200°C.

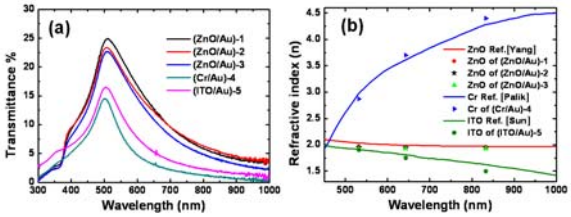

Figure 3. Measurement of the optical properties and surface morphology (a) The transmittance spectrum of each sample. (b) The measured refractive index of samples (symbol) compared with the data from published literature (solid line).

3.3.Chemical detection

SPR reflectivity curves were measured in angular interrogation mode using an imaging ellipsometric platform EP³ SPR system. In intensity interrogation mode SPR, the real-time reflectance intensity was measured. The experimental results shown in Fig. 4(a) illustrate the performance of SPR devices in ethanol solutions of weight percentages 0% (deionized water), 1.25%, 2.5%, 5%, 10% and 20%. Comparison of the real-time monitoring of the ethanol signals shows that the (ZnO/Au)-1 device (red line) exhibits a shorter transition time and higher steady-state response compared to a traditional (Cr/Au)-4 (green line) and (ITO/Au)-5 (blue line). A comparison of the measured reflectance intensity shift relationships between the (ZnO/Au)-1 and (Cr/Au)-4 devices, in 1.25%, 2.5%, 5%, 10% and 20% ethanol yield relative values of 4.5, 3.7, 2.7, 1.9 and 1.7-fold at a signal-to-noise ratio of 9:1. Fig. 4(b) shows that the experimentally-determined SPR characteristics in intensity interrogation mode exhibited a good agreement with the calibration curve. The (ZnO/Au)-1 device gave a linear plot for the range 0% to 20%, with a linear regression equation y = 10.74x – 1.1, and correlation coefficient (R^2) of 0.991, where y represents the reflectance intensity (a.u.) and x the ethanol concentration. In addition, the linear regressions of the calibration curves were y=4.36x−1.85, with a correlation coefficient R^2 = 0.934, for the (Cr/Au)-4 device and y=6.67x−1.15, with a correlation coefficient R^2 = 0.968, for the (ITO/Au)-5 device.

Fig. 4(c) shows that the SPR response measurement results for the calibration curves obtained for deionized water (0%), and for 1.25%, 2.5%, 5% 10%, 20%, 30%, 40%, 50%, 60%, 70%, 80%, and 95 % ethanol concentration (as weight percentage). Fig. 4(d) shows that the SPR responses to the corresponding average inaccuracy of SPR angles were ±0.018°, ±0.021°, and ±0.021° (n=3) for the (ZnO/Au)-1, (Cr/Au)-4 and (ITO/Au)-5 devices,

respectively. The experimental data gave good agreement when fitted to the calibration curve. In our sample devices, the linear regression of the calibration curve was y =146.62x −146.33 (correlation coefficient, R^2 = 0.998) for (ZnO/Au)-1, y=100.73x−84.54 (correlation coefficient, R^2 = 0.986) for (Cr/Au)-4, and y=107.11x−92.83 (correlation coefficient, R^2 = 0.985) for (ITO/Au)-5, where x is the refractive index unit (RIU) and y is the SPR angle (θ).

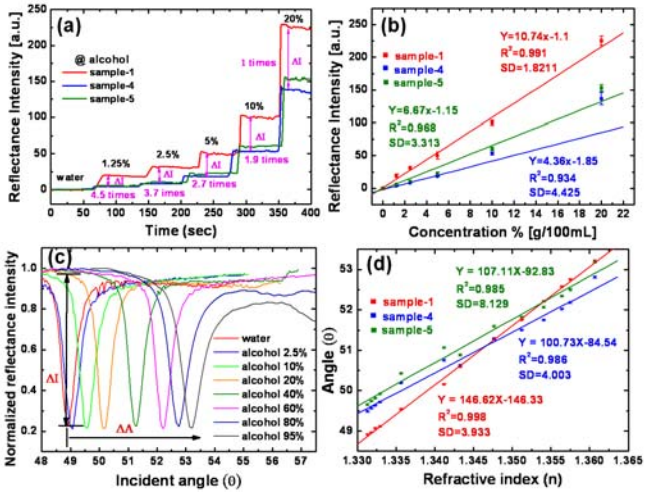

Figure 4. Comparison of the SPR reflectivity curves obtained at different concentrations of ethanol. (a) Real-time monitoring of the response of the (ZnO/Au)-1, (Cr/Au)-4 and (ITO/Au)-5 devices in water (0%) and in 1.25%, 2.5%, 5%, 10% and 20% ethanol solutions. (b) Linear regression of the sensing experimental data over the dynamic range of 0% to 20%. (c) Angular interrogation mode measurement results obtained for the (ZnO/Au)-1 device in water and ethanol solutions. (d) The calibration curve for the determination of water and ethanol for the (ZnO/Au)-1, (Cr/Au)-4 and (ITO/Au)-5 devices.

4 CONCLUSIONS

The observation of an SPR effect caused by an intermediary layer of ZnO thin film extends the application of plasmons to a new range of biosensors. We varied the device fabrication parameters to demonstrated that ZnO (002) crystalline quality can enhance the SPR mechanism. Crystalline quality is the most important deposition parameter relating thin film density to the refractive index. In this study using ATR based on a Prism/Glass/ZnO/Au configuration coupled with a high refractive index (1.96) and high transparency (90%) ZnO intermediary layer, we show an improvement in the FWHM of the SPR reflectivity curve.

ACKNOWLEDGEMENTS:

This project is supported in part by National Science and Technology Program in Pharmaceuticals and Biotechnology, National Science Council, Taiwan, R.O.C., NSC 96-2218-E-002-026, NSC 97-2218-E-002-014, NSC 98-2221-E-002-038-MY3, and NSC 99-2218-E-003-002-MY3.

REFERENCES

1. H. Raether, Surface Plasmons on Smooth and Rough Surfaces and on Gratings, Springer Tracts Mod. Phys. 111, 1, Verlag, Berlin, (1988).
2. A. Otto, Zeitschrift f˙ur Physik 216, 398 (1968).
3. E. E. Kretschmann and H. Raether, Z. Naturforsch 23 2135-2136(1968).
4. R. W. Wood, Proc. of the Physical Society of London 18 269-275(1902).
5. W. P. Chen, J.M. Chen, J. Opt. Soc. Am. 71, 189-191(1981).
6. J. Homola, S. S. Yee, and G. Gauglitz, Sens. Actuators B 54, 3-15(1999).
7. R. Rella, J. Spadavecchia, M. G. Manera, P. Siciliano, A. Santino and G. Mita, Biosens. Bioelectron. 20, 1140-1148(2004).
8. Y. Wang and W. Knoll, Anal. Chim. Acta 558, 150-157(2006).
9. S. Chah, C. V. Kumar, M. R. Hammond and R. N. Zare, Anal. Chem. 76, 2112-2117 (2004).
10. P. H. Holloway, Gold Bull., 12, 99-106(1979).
11. H. Neff, W. Zong, A.M.N. Lima, M. Borre, G. Holzhuter, Thin Solid Films 496, 688 – 697(2006).
12. N.-F. Chiu, C.-W. Lin, J.-H. Lee, C.-H. Kuan, K.-C. Wu and C.-K. Lee, Appl. Phys. Lett. 91, 083114 (2007).
13. N.-F. Chiu, C. Yu, J.-H. Lee, C.-H. Kuan, K.-C. Wu, C.-K. Lee, C.-W. Lin, Opt. Express. 15, 11608(2007).
14. S.-Y. Nien, N.-F. Chiu, Y.-H. Ho, J.-H. Lee, C.-W. Lin, K.-C. Wu, C.-K. Lee, J.-R. Lin, M.-K. Wei, and T.-L. Chiu, Appl. Phys. Lett. 94, 103304(2009).
15. C. J. Alleyne, A. G. Kirk, R. C. McPhedran, N.-A. P. Nicorovici and D. Maystre, Opt. Express 15, 8163-8169(2007).
16. C.-W. Lin, K.-P. Chen, S.-M. Lin, C.-K. Lee, Sens. Actuators B 113, 169-176 (2006).
17. S. Patskovsky, S. Bah, M. Meunier, and A. V. Kabashin, Appl. Opt. 45, 6640-6645 (2006).
18. C. Rhodes, and S. Franzen, J.-P. Maria, M.Losego, D. N. Leonard, B. Laughlin, G. Duscher, and S. Weibel, J. Appl. Phys. 100, 054905 (2006).
19. S.Franzen, J. Phys. Chem. C 112, 6027-6032(2008).
20. Ü. Özgür, Y. I. Alivov, C. Liu, A. Teke, M. A. Reshchikov, S. Doğan, V. Avrutin, S. J. Cho and H. Morkoc, J. Appl. Phys. 98, 041301 (2005).
21. A. B. Djurišić, Y. H. Leung, Small 2, 944-961(2006).
22. H. Liao, W. Wen, G. K. Wong, and G. Yang, Opt. Lett. 28, 1790-1792(2003).
23. X. Wang, X. Kong, Y. Yu, H. Zhang, J. Phys. Chem. C 111, 3836–3841(2007).
24. H. L. Mosbacker, Y. M. Strzhemechny, B. D. White, P. E. Smith, D. C. Look, D. C. Reynolds, C. W. Litton, L. J. Brillson, Appl. Phys. Lett. 87, 012102-012103 (2005).
25. L. Wang, J. Wang, S. Zhang, Y. Sun, X. Zhu, Y. Cao, X. Wang, H. Zhang, D. Song, Analytica Chimica Acta 653, 109–115(2009).
26. C.-C. Chang, N.-F. Chiu, D. S. Lin, S.-Y. Chu, and C.-W. Lin, Anal. Chem., 82, 1207–1212(2010).
27. A. I. Usoskin, and I. N. Shklyarevskii, Zhurnal Prikladnoi Spektroskopii, 20, 523-524 (1974).
28. E. D. Palik, Handbook of Optical Constants of Solids. Academic Press, New York. (1991).
29. C. W. Lai, J. An, and H. C. Ong, Appl. Phys. Lett., 86, 251105(2005).
30. J. Herrero, and C. Guillen, Thin Solid Films 451-452, 630–633(2004).
31. C. Guillen, and J. Herrero, Thin Solid Films 480-481, 129-132(2005).
32. X. Yan, F.W. Mont, D. J. Poxson, M. F. Schubert, J. K. Kim, J. Cho, and E. F. Schubert, Jpn. J. Appl. Phys. 48, 120203(2009).
33. D.-S. Wang and C.-W. Lin, Opt. Lett. 32, 2128–2130(2007).
34. Y. Yang, X.W. Sun B.J. Chen, C.X. Xu, T.P. Chen, C.Q. Sun, B.K. Tay, Z. Sun, Thin Solid Films 510, 95 – 101(2006).
35. X. W. Sun, H. S. Kwok, J. Appl. Phys. 86, 408-411(1999).